

## Cascaded erenkov third-harmonic generation in random quadratic media

Mousa Ayoub, Philip Roedig, Jörg Imbrock, and Cornelia Denz

Citation: *Appl. Phys. Lett.* **99**, 241109 (2011); doi: 10.1063/1.3670322

View online: <http://dx.doi.org/10.1063/1.3670322>

View Table of Contents: <http://apl.aip.org/resource/1/APPLAB/v99/i24>

Published by the [American Institute of Physics](#).

---

### Related Articles

Time-resolved femtosecond optical characterization of multi-photon absorption in high-pressure-grown  $\text{Al}_{0.86}\text{Ga}_{0.14}\text{N}$  single crystals

*J. Appl. Phys.* **110**, 113112 (2011)

Experimental observation of optical vortex in self-frequency-doubling generation

*Appl. Phys. Lett.* **99**, 241102 (2011)

Model for nanosecond laser induced damage in potassium titanyl phosphate crystals

*Appl. Phys. Lett.* **99**, 231111 (2011)

Direct comparison of phase-sensitive vibrational sum frequency generation with maximum entropy method: Case study of water

*J. Chem. Phys.* **135**, 224701 (2011)

Continuous-wave cascaded-harmonic generation and multi-photon Raman lasing in lithium niobate whispering-gallery resonators

*Appl. Phys. Lett.* **99**, 221111 (2011)

---

### Additional information on *Appl. Phys. Lett.*

Journal Homepage: <http://apl.aip.org/>

Journal Information: [http://apl.aip.org/about/about\\_the\\_journal](http://apl.aip.org/about/about_the_journal)

Top downloads: [http://apl.aip.org/features/most\\_downloaded](http://apl.aip.org/features/most_downloaded)

Information for Authors: <http://apl.aip.org/authors>

### ADVERTISEMENT

The logo for AIP Advances features the text 'AIPAdvances' in a blue and green font. Above the text is a decorative graphic of several orange circles of varying sizes, some of which are connected by a dotted line.

*Submit Now*

**Explore AIP's new  
open-access journal**

- **Article-level metrics  
now available**
- **Join the conversation!  
Rate & comment on articles**

# Cascaded Čerenkov third-harmonic generation in random quadratic media

Mousa Ayoub,<sup>a)</sup> Philip Roedig, Jörg Imbrock, and Cornelia Denz

*Institute of Applied Physics and Center for Nonlinear Science (CeNoS), Westfälische Wilhelms-Universität Münster, Corrensstraße 2, 48149 Münster, Germany*

(Received 16 September 2011; accepted 25 November 2011; published online 14 December 2011)

We investigate experimentally and theoretically the conical emission of Čerenkov-type third-harmonic generation in strontium barium niobate of random 2D- $\chi^{(2)}$  distribution. The azimuthal intensity distribution is explained by the polarization properties of the fundamental and Čerenkov second-harmonic waves, depending on the cascaded origin of the generation process. Moreover, we show the role of the individual domain shape in an additional modulation on the conical emission, controlled by the electrical switching of the spontaneous polarization of the ferroelectric medium. © 2011 American Institute of Physics. [doi:10.1063/1.3670322]

Multistep parametric interactions and multistep cascading effects in optical materials with second-order nonlinear response represent an efficient type of parametric processes that are characterized by at least two different phase-matched processes; second-harmonic generation (SHG) and sum-frequency mixing (SFM).<sup>1,2</sup>

The efficiency of these parametric processes relies on the phase-velocity synchronization of the generated waves.<sup>3</sup> The generation of new frequencies can be experimentally achieved depending on the phase-matching configuration as, for example, birefringence-induced phase matching or quasi-phase matching (QPM) in one as well as two dimensions.<sup>4,5</sup> Recently, much attention has been devoted to the investigation of various schemes of random quasi-phase matching in crystals with irregular domain structures due to their potential benefits for nonlinear parametric processes for different characteristic noncollinear emissions.<sup>6–9</sup> Cascaded processes have also been observed and studied, e.g., cascaded third harmonic generation (THG) in quasi-random media.<sup>10</sup> Among the most interesting emission processes is the so-called Čerenkov scheme, where the phase velocity of the nonlinear polarization wave driven by the fundamental wave is faster than that of the harmonic.<sup>11–14</sup> Moreover, the observation of conical cascaded Čerenkov-type third harmonic generation in LiNbO<sub>3</sub> was recently reported with artificially disordered square domain lattices.<sup>15</sup> However, up to now, no third harmonic (TH) conical emission was experimentally reported in totally randomized crystals due to the low conversion efficiency.

In this work, we report quantitatively both on the experimental and theoretical analysis of Čerenkov third-harmonic emission in random strontium barium niobate (SBN). We analyze the role of both, the polarization properties of the  $\chi^{(2)}$  tensor and of the domain size and shape of fourfold symmetry corresponding to the crystal symmetry 4 mm of SBN.<sup>14,16</sup>

In our experiments, we study the conical emission of third-harmonic generation of ultrashort laser pulses in SBN with different domain shapes. The individual domain shape is strongly influenced by homogeneously electrical domain switching at room temperature. As reported in Ref. 14,

domain switching leads to fourfold modulation on the SH cone. It has been pointed out that this modulation cannot be attributed to the polarization properties of the nonlinear tensor of SBN. In this work, we will show that the TH cone has not only the fourfold symmetry due to the domain shape as in the case of SH cone but also an additional modulation coming from the polarization superposition of the SH cone and the fundamental waves. Thus, the polarization properties of the TH cone clearly show the cascaded origin of this process. In our calculations, we apply the Green's function approach,<sup>13,14,17</sup> using the corresponding phase-matching condition and compare with the experiments. The opening angle over a wide wavelength range is also examined and confirmed theoretically.

In the experiment, we use an Sr<sub>0.61</sub>Ba<sub>0.39</sub>Nb<sub>2</sub>O<sub>6</sub> crystal with the dimensions 6.6 × 6.6 × 1.6 mm<sup>3</sup>. The large surface perpendicular to the optical axis is polished to optical quality. The sample was heated up above Curie temperature  $T_c \approx 70$ –80 °C followed by cooling down without applying an electric field for erasing any spurious polarization. To overcome the problem of the low conversion efficiency, the sample was poled and repoled at room temperature to enhance the TH signal but the random nature of the medium is still preserved<sup>9,14</sup> [see Fig. 1(a)]. We use ultrashort laser pulses with a pulse duration of about 80 fs and a repetition rate of 1 kHz. The pulse energy amounts to 100 μJ,

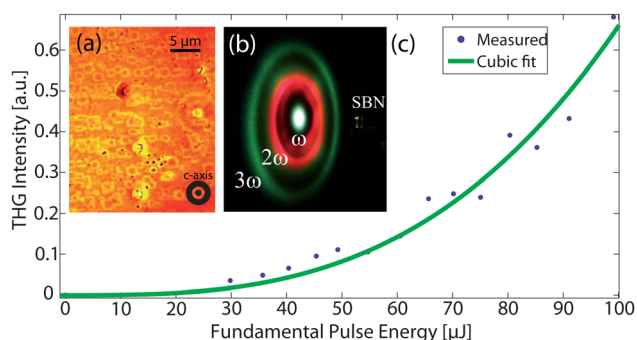


FIG. 1. (Color online) (a) Phase contrast image of a polydomain crystal looking through the surface perpendicular to the c-axis. (b) Experimental photograph of the TH and SH conical emission at 1600 nm input wavelength. (c) Power of the third harmonics vs. the input power of the fundamental beam. Solid line represents a cubic fit.

<sup>a)</sup>Electronic mail: ayoubm@uni-muenster.de.

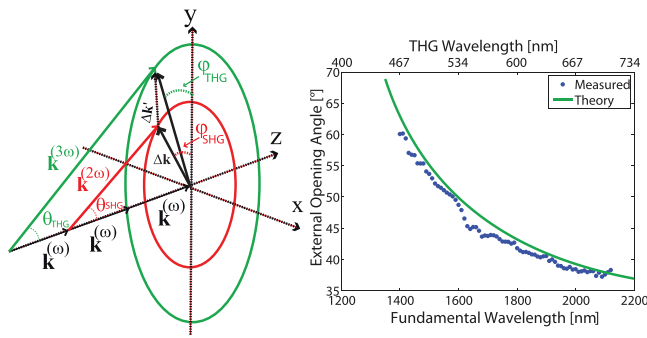


FIG. 2. (Color online) (a) Diagram of the longitudinal phase matching for cascaded third-harmonic generation.  $\Delta k$  and  $\Delta k'$  are the corresponding phase mismatches. (b) Measured TH opening angle over a wide wavelength range. The solid curve represents the numerical calculations.

depending on the wavelength, which is tuned in the experiments between  $\lambda = 1400$  and  $2120$  nm. The laser beam is slightly focused, linearly polarized, and propagates along the  $c$ -axis of the sample. The SH and TH signals are emitted on cones in the far-field as shown in Fig. 1(b). It is worth to note that no third-harmonic signal was observed in a mono-domain crystal.

Fig. 1(b) shows experimental photographs of the SH and TH conical emissions at  $\lambda = 1600$  nm. The plot in Fig. 1(c) depicts the measured dependence of the energy of the third harmonic as a function of the power of the fundamental beam. As expected, the experimental points follow faithfully the cubic fit. The opening angle of TH cone in turn obeys the corresponding longitudinal phase-matching condition [see Fig. 2(a)]:  $\mathbf{k}^{(2\omega)} - 2\mathbf{k}^{(\omega)} = \Delta\mathbf{k}$  for SHG and  $\mathbf{k}^{(3\omega)} - \mathbf{k}^{(\omega)} - \mathbf{k}^{(2\omega)} = \Delta\mathbf{k}'$  for THG, where  $\mathbf{k}^{(\omega)}$ ,  $\mathbf{k}^{(2\omega)}$ , and  $\mathbf{k}^{(3\omega)}$  are the wave vectors of the fundamental, second harmonic, and third harmonic waves, respectively. The phase mismatches of the SHG and THG processes are denoted by  $\Delta\mathbf{k}$  and  $\Delta\mathbf{k}'$ , respectively. In analogy to the SH cone, considering the cascaded nature of this process, the opening angle is ruled by the following equation:  $k^{(3\omega)} \cos \theta_{\text{THG}} = k^{(\omega)} + k^{(2\omega)} \cos \theta_{\text{SHG}} = 3k^{(\omega)}$ . Experimentally, the TH opening angle is measured for fundamental waves from  $\lambda = 1400$  nm to  $\lambda = 2120$  nm. The results are depicted in Fig. 2(b). In good agreement with the calculation (solid line), the opening angle becomes smaller for larger wavelengths. No TH cone was observed for wavelengths smaller than  $\lambda = 1320$  nm because of the total reflection of the TH wave inside the SBN sample.

In the next experiment, we analyze the polarization properties of both TH and SH cones. A linear polarizer is set behind the sample and rotated [Fig. 3]. The TH cones are radially polarized as can be seen in Fig. 3 for several angles

of output polarization. As shown, the positions of the maximal intensity of the second and third harmonics depend on the orientation of the output polarization.

In addition to the fourfold modulation caused by the individual domain shape,<sup>14</sup> the overlap of the second-harmonic and the linear fundamental polarizations leads to an intensity modulation on the TH cone. For instance, for a vertical input polarization, a cancellation of the TH signal is expected at the horizontal plane [see Fig. 4(a)], because the fundamental and second harmonic waves are perpendicularly polarized to each other at the horizontal plane. This filtering effect of the SH cone obviously clarifies the cascaded generation of the TH cone. Figure 4 (top row) shows three different intensity maxima positions for different input polarization orientations and the corresponding azimuthal intensity profiles of the TH cone for each case (middle row). The dominant intensity peaks representing the four-fold modulation are marked with dashed red lines. The role of the domain shape can also be clearly seen in Fig. 4. Four characteristic TH intensity peaks representing the fourfold symmetry of the individual domains in SBN appear at fixed places with similar behavior of the SH cone. However, these peaks can be partially eliminated depending on the input polarization as in Fig. 4(b).

We recall that the formation of the third harmonic in our case is a combination of two processes: Second-harmonic generation and sum frequency generation  $3\omega = \omega + 2\omega$ . Therefore, the driven polarization will be:  $\mathbf{P}^{(3\omega)}(\mathbf{r}) \propto \epsilon_0 \hat{d}_{\text{eff}}^{(2)} \mathbf{E}^{(\omega)} \mathbf{E}^{(2\omega)}$ , where  $\hat{d}_{\text{eff}}^{(2)}$  is the corresponding effective nonlinearity. Applying the Green's function approach,<sup>17</sup> the third harmonic field can be recast as follows:  $\mathbf{E}^{(3\omega)}(\mathbf{r}) \propto \int_{V_{\text{NL}}} d\mathbf{r}' \hat{\mathbf{G}}(\mathbf{r}, \mathbf{r}') \mathbf{P}^{(3\omega)}(\mathbf{r}')$ , where  $V_{\text{NL}}$  is the nonlinear domain volume and  $\hat{\mathbf{G}}(\mathbf{r}, \mathbf{r}')$  is the dyadic Green's function which can be obtained from the scalar Green's function of a three-dimensional homogeneous medium.<sup>17</sup> The far-field intensity can then be easily calculated from:  $I^{(3\omega)} \propto |\mathbf{E}^{(3\omega)}(\mathbf{r})|^2$ . Taking into account the polarization properties of the interacting beams and the involved nonlinear coefficients of SBN, the effective nonlinear coefficients are  $d_{\text{eff}}^e = d_{31} \cos \varphi_0 \cos \theta_{\text{SHG}} \cos \varphi_{\text{SHG}} + d_{32} \sin \varphi_0 \cos \theta_{\text{SHG}} \sin \varphi_{\text{SHG}}$ ,  $d_{\text{eff}}^{o,x} = d_{15} \cos \varphi_0 \sin \theta_{\text{SHG}}$ , and  $d_{\text{eff}}^{o,y} = d_{24} \sin \varphi_0 \sin \theta_{\text{SHG}}$ , where  $\varphi_0$  is the input polarization orientation and  $\varphi_{\text{SHG}}$  is the azimuthal angle of the SH cone, respectively.

Due to the fact that the TH-field at a certain  $\varphi_{\text{THG}}$  is an overlap of all SH-field components with the fundamental field, the total TH-field will be  $E_{\text{tot}}^{(3\omega)}(\theta_{\text{THG}}, \varphi_{\text{THG}}) \propto \int_0^{2\pi} d\varphi_{\text{SHG}} d_{\text{eff}}(\varphi_{\text{SHG}}) \int_{V_{\text{NL}}} d^3r' \exp(-i\Delta\mathbf{k}'(\varphi_{\text{SHG}})\mathbf{r}')$ . The numerical simulations were done with a nonlinear medium  $V_{\text{NL}}$  which has a 3D parallelepiped shape with a height  $h$  along the  $z$ -axis,

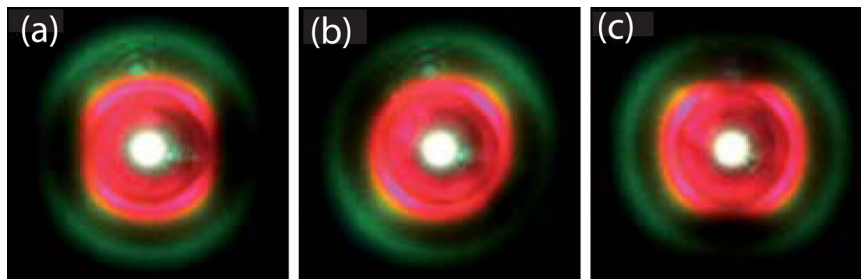


FIG. 3. (Color online) Experimental photographs recorded for different output polarization angles of the third harmonic wave. (a) to (c)  $0^\circ$ ,  $45^\circ$ , and  $90^\circ$ , respectively.



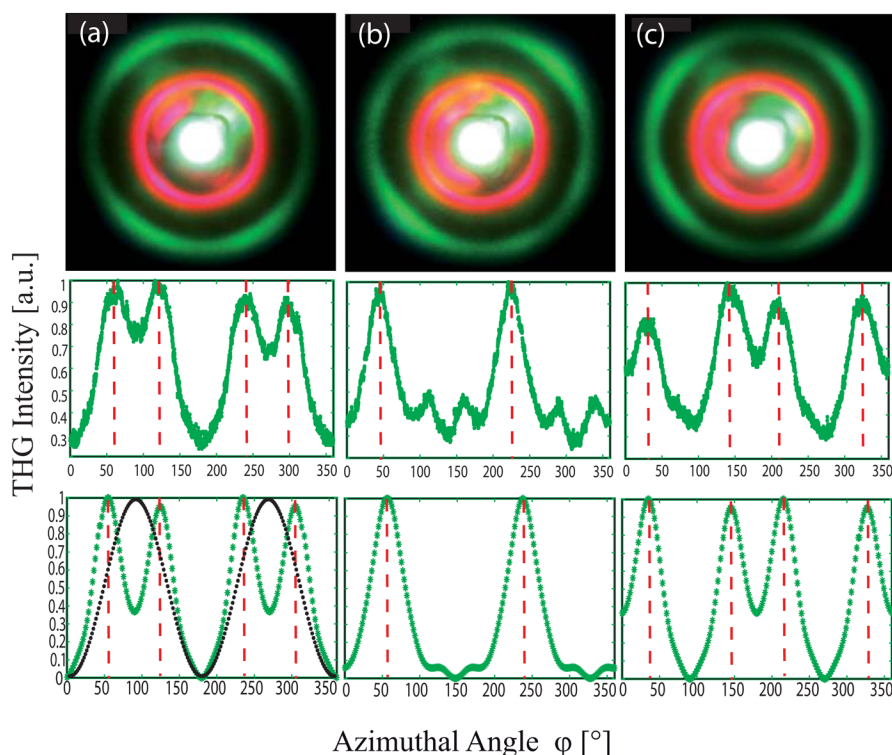


FIG. 4. (Color online) Experimental photographs (top row) recorded for different input polarization angles of the fundamental wave. (a) to (c)  $\phi_0 = 0^\circ$ ,  $44^\circ$ , and  $92^\circ$ , respectively. (middle row): The corresponding azimuthal intensity profiles. (bottom row): Numerical simulations of the azimuthal intensity distribution for large domains (marked with vertical-dashed lines) and small domains (non-marked). The absolute THG intensity for small domains is about two orders of magnitude smaller than for large domains.

diameter  $d$ , and a square cross section with rounded corners.<sup>14,16</sup> We have applied this model for two different characteristic sizes of the ferroelectric domains in SBN. For the unpoled case,<sup>9</sup> ferroelectric domain widths are between  $d = 150$  nm and  $400$  nm and a height  $h = 7$   $\mu$ m. No TH signal was measurable in the experiment. Therefore, we show our numerical prediction for this domain size. The results show the modulation which is based only on the input polarization orientation as in Fig. 4 (bottom row) (non-marked curve). However, the role of the domain shape begins to arise when the ferroelectric domains become broader, i.e., when poling and repoling the crystal stepwise at room temperature in the same manner as in Refs. 9 and 14. For the repoled case, we chose  $d = 1.7$   $\mu$ m and  $h = 20$   $\mu$ m [see Fig. 1(a)]. The theoretical azimuthal intensity distribution is exemplarily depicted in Fig. 4 (bottom row), in which the effect of the squareness of the individual domain is also marked by red dashed lines in good agreement with the experimental results. Moreover, the calculations predict that the SH as well as the TH intensity average increases with increasing domain width  $d$ . Thus, for the repoled case, the TH intensity is about two orders of magnitude larger than for the unpoled case. Finally, it is worth to note that this one-domain model shows the ability to describe this process in random media due to the incoherent overlap of the SH and TH signals emitted from all domains which are randomly distributed in such as medium for this configuration.

In conclusion, we have studied experimentally and numerically the conical emission of the third harmonic generation in a random nonlinear medium with a crystal symmetry of 4mm. We analyzed the cascaded generation depending on the polarization properties of the second harmonic and the fundamental waves. The TH opening angle

was experimentally measured over a wide wavelength range. As shown, the polarization combination leads to an additional modulation on the TH cone. Furthermore, the role of the domain shape is easily observable when ferroelectric domains grow with help of the electrically switching of the domains. We numerically reproduced the TH patterns in good agreement with the experiment, taking into account both polarization and domain shape properties.

<sup>1</sup>S. M. Saltiel, A. A. Sukhoroukov, and Y. S. Kivshar, *Prog. Opt.* **47**, 1 (2005).

<sup>2</sup>R. Ivanov and S. Saltiel, *J. Opt. Soc. Am. B* **22**, 1691 (2005).

<sup>3</sup>J. A. Armstrong, N. Bloembergen, J. Ducuing, and P. S. Pershan, *Phys. Rev.* **127**, 1918 (1962).

<sup>4</sup>V. Berger, *Phys. Rev. Lett.* **81**, 4136 (1998).

<sup>5</sup>A. Arie, N. Habshoosh, and A. Bahabad, *Opt. Quantum Electron.* **39**, 361 (2007).

<sup>6</sup>A. R. Tunyagi, M. Ulex, and K. Betzler, *Phys. Rev. Lett.* **90**, 243901 (2003).

<sup>7</sup>K. A. Kuznetsov, G. K. Kitaeva, A. V. Shevlyuga, L. I. Ivleva, and T. R. Volk, *JETP Lett.* **87**, 98 (2008).

<sup>8</sup>P. Molina, S. Á. García, M. O. Ramírez, J. García-Solé, L. E. Bausá, H. Zhang, W. Gao, J. Wang, and M. Jiang, *Appl. Phys. Lett.* **94**, 071111 (2009).

<sup>9</sup>M. Ayoub, J. Imbrock, and C. Denz, *Opt. Express* **19**, 11340 (2011).

<sup>10</sup>Y. Sheng, S. M. Saltiel, and K. Koynov, *Opt. Lett.* **34**, 656 (2009).

<sup>11</sup>K. Hayata, H. Matsumura, and M. Koshiba, *J. Appl. Phys.* **70**, 1157 (1991).

<sup>12</sup>S. M. Saltiel, Y. Sheng, N. Voloch-Bloch, D. N. Neshev, W. Krolikowski, A. Arie, K. Koynov, and Y. S. Kivshar, *IEEE J. Quantum Electron.* **45**, 11 (2009).

<sup>13</sup>J. Bravo-Abad, X. Vidal, J. L. D. Jurez, and J. Martorell, *Opt. Express* **18**, 14202 (2010).

<sup>14</sup>M. Ayoub, P. Roedig, J. Imbrock, and C. Denz, *Opt. Lett.* **36**, 4371 (2011).

<sup>15</sup>Y. Sheng, W. Wang, R. Shiloh, V. Roppo, Y. Kong, A. Arie, and W. Krolikowski, *Appl. Phys. Lett.* **98**, 241114 (2011).

<sup>16</sup>L. Tian, D. A. Scrymgeour, and V. Gopalan, *J. Appl. Phys.* **97**, 114111 (2005).

<sup>17</sup>J. Cheng and X. Xie, *J. Opt. Soc. Am. B* **19**, 1604 (2002).